AGU PUBLICATIONS

Geophysical Research Letters

RESEARCH LETTER

10.1002/2015GL065814

Key Points:
- Eddy-Kuroshio interaction is observed with 11 pressure sensor-equipped inverted echo sounders
- Eddy-influence weakens across the Kuroshio east of Taiwan and northeast of Luzon
- Eddy-influence causes seesaw-like SSHa changes across the Kuroshio most obviously east of Taiwan

Supporting Information:
- Figure S1 and Tables S1 and S2

Correspondence to:
M. Andres and S. Jan,
mandres@whoi.edu;
senjan@ntu.edu.tw

Citation:
Tsai, C.-J., M. Andres, S. Jan, V. Mensah, T. B. Sanford, R.-C. Lien, and C. M. Lee (2015), Eddy-Kuroshio interaction processes revealed by mooring observations off Taiwan and Luzon, *Geophys. Res. Lett.*, *42*, 8098–8105, doi:10.1002/2015GL065814.

Received 17 AUG 2015
Accepted 17 SEP 2015
Accepted article online 23 SEP 2015
Published online 8 OCT 2015

Eddy-Kuroshio interaction processes revealed by mooring observations off Taiwan and Luzon

Cheng-Ju Tsai[1], Magdalena Andres[2], Sen Jan[1], Vigan Mensah[1], Thomas B. Sanford[3], Ren-Chieh Lien[3], and Craig M. Lee[3]

[1]Institute of Oceanography, National Taiwan University, Taipei, Taiwan, [2]Woods Hole Oceanographic Institution, Woods Hole, Massachusetts, USA, [3]Applied Physics Laboratory, University of Washington, Seattle, Washington, USA

Abstract The influence and fate of westward propagating eddies that impinge on the Kuroshio were observed with pressure sensor-equipped inverted echo sounders (PIESs) deployed east of Taiwan and northeast of Luzon. Zero lag correlations between PIES-measured acoustic travel times and satellite-measured sea surface height anomalies (SSHa), which are normally negative, have lower magnitude toward the west, suggesting the eddy-influence is weakened across the Kuroshio. The observational data reveal that impinging eddies lead to seesaw-like SSHa and pycnocline depth changes across the Kuroshio east of Taiwan, whereas analogous responses are not found in the Kuroshio northeast of Luzon. Anticyclones intensify sea surface and pycnocline slopes across the Kuroshio, while cyclones weaken these slopes, particularly east of Taiwan. During the 6 month period of overlap between the two PIES arrays, only one anticyclone affected the pycnocline depth first at the array northeast of Luzon and 21 days later in the downstream Kuroshio east of Taiwan.

1. Introduction

Outside of a narrow region straddling the equator, westward propagating coherent features are ubiquitous throughout the world's oceans. These are readily apparent in time series of mapped sea surface height anomalies (SSHa) from satellite altimetry and have been interpreted as expressions of baroclinic linear Rossby waves [e.g., *Qiu*, 2003] and nonlinear eddies [e.g., *Chelton et al.*, 2007].

Cyclonic and anticyclonic mesoscale features from the ocean interior, collectively termed eddies here, arrive frequently in the western North Pacific—particularly east of Luzon [*Lien et al.*, 2014] and Taiwan [*Yang et al.*, 1999] where they impinge on the northward flowing Kuroshio (Figure 1) at 100 day interval [*Zhang et al.*, 2001; *Johns et al.*, 2001; *Yang et al.*, 1999]. Observational results indicate the existence of eddy-Kuroshio interactions in which the Kuroshio affects eddies (which in altimetry appear to decay near the western boundary) and also interactions in which eddies drive Kuroshio variability [e.g., *Lien et al.,* 2014; *Andres et al.*, 2008a]. A reduced-gravity, primitive equation model [*Chern and Wang*, 2005; *Kuo and Chern*, 2011] suggests that an idealized circular eddy deforms and decays quickly when it moves into a western boundary current (WBC). However, these idealized simulations have yet to be evaluated against in situ observations.

Comparison of sea surface height (SSH) variability with temperature and salinity profiles from Argo floats shows that SSH is generally well correlated with dynamic height in the interior ocean [*Guinehut et al.*, 2009] where positive SSH anomaly (SSHa) at eddy timescales often corresponds with a depressed pycnocline (due to convergence in the upper layers), while negative SSHa corresponds with a heaved pycnocline (due to divergence in the upper layers). Because the global Argo fleet undersamples WBCs and the variability of eddies is often aliased in shipboard conductivity-temperature-depth (CTD) and expendable bathythermograph observations, it is not yet well established whether these relationships at eddy timescales also hold true near western boundaries and across strong currents.

Altimetry is not sufficient to fully characterize WBC/eddy interactions, because spacing between Jason-2 altimeter tracks can be greater than 300 km in the subtropics and the repeat cycle is about 10 days. Furthermore, although SSH gradients are associated with the surface geostrophic velocities (which may be related to deeper geostrophic velocities), they provide no *direct* information about the deep circulation or pycnocline displacements associated with eddies.

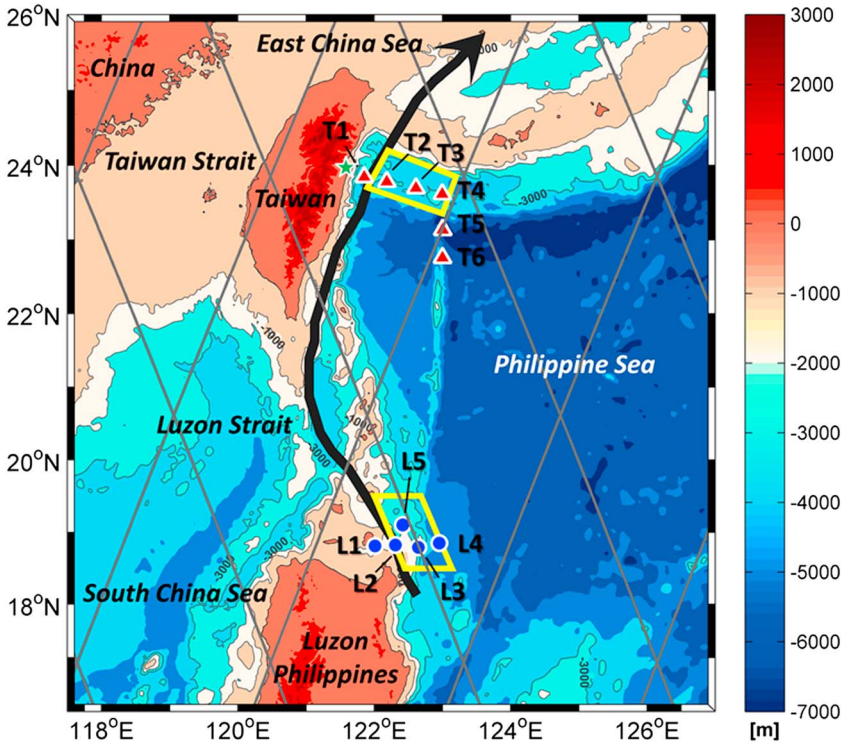

Figure 1. Bathymetry around Taiwan and Luzon (shaded) with the mean position of Kuroshio maximum velocity at 15 m depth (black arrow) as derived from the surface drifter data (available at http://www.coriolis.eu.org), locations of PIESs northeast of Luzon (blue circles), east of Taiwan (red triangles), and Haulien tide station (green star), and the 1000 m, 2000 m and 3000 m isobaths. Historical CTD data in the two regions bounded by yellow lines are used to interpret the PIES data and are chosen to include sufficient casts to find a robust empirical relationship without including water masses from neighboring regions.

To understand WBC/eddy interactions, it is helpful to anchor the remote sensing measurements with in situ observations. Two such in situ arrays were recently deployed across the Kuroshio in the western North Pacific [*Lien et al.*, 2014; Andres et al., unpublished data] and included observations made using pressure sensor-equipped inverted echo sounders (PIESs) deployed at zonal transects across the Kuroshio: one PIES array northeast of Luzon and another about 300 km downstream, east of Taiwan. Using these data augmented with satellite SSHa, the primary objective of this study is to evaluate the temporal and spatial ranges of eddies' influence on pycnocline depth variations across the Kuroshio and on the latitudinal connectivity of Kuroshio variability.

2. Data and Methods

Two companion programs, Origins of the Kuroshio and Mindanao Current (OKMC) sponsored by the U.S. Office of Naval Research and Observations of the Kuroshio Transports and their Variability (OKTV) sponsored by the Ministry of Science and Technology of Taiwan, aimed at understanding Kuroshio variability [*Lien et al.*, 2014; *Jan et al.*, 2015]. OKMC-OKTV field programs included 11 PIESs deployed across the Kuroshio (Table S1). PIESs measure round-trip acoustic travel time (τ) between the instrument (moored on the seabed) and the overlying sea surface [*Watts and Rossby*, 1977]. Both sound speed and specific volume anomaly (δ) depend on temperature, salinity, and pressure, and in a given region τ can be used as a proxy for a vertical profile of δ with the relationship between τ and δ established empirically with local hydrographic measurements [e.g., *Meinen*, 2001; *He et al.*, 1998]. To estimate both the baroclinic (steric) component of SSHa and pycnocline depth, d_{pyc}, τ has been used [*Andres et al.*, 2008b; *Baker-Yeboah et al.*, 2009]. Here τ', the deviation of τ from its time mean, is used to examine the relationship between the Kuroshio variability and impinging eddies at the two PIES arrays. Based on the global relationships between SSHa and pycnocline depth observed with Argo

floats and the temperature and salinity dependence of sound speed, a negative correlation between SSHa and τ' at the PIES sites is anticipated.

Under OKTV, six PIESs were deployed east of Taiwan from 14 November 2012 to 30 October 2014 (Figure 1, red triangles), with four located along ~23.75°N between 121.85°N and 123°E at 50 km interval and two deployed along 123°E between 22.76°N and 23.14°N. Under the companion OKMC program, five PIESs (Figure 1, blue circles) were deployed northeast of Luzon along 18.82°N between 122.01°E and 122.95°E at 30 km interval from June 2012 to June 2013, with one instrument offset 30 km to the north.

Concurrent SSHa from the 1/4° gridded altimetry product that merges measurements from all available satellites was obtained from Ssalto/Duacs and distributed by Archiving, Validation and Interpretation of Satellite Oceanographic data (AVISO, http://www.aviso.oceanobs.com).

To quantify the influence of impinging eddies on the Kuroshio's pycnocline, time series of d_{pyc} at each PIES site are inferred from hourly τ measurements that have been 30 day low pass filtered and converted to a common reference level, 800 dbar, τ_{800} using the procedure described in *Kennelly et al.* [2007]. The relationships between d_{pyc} and τ_{800} are determined empirically for each PIES array using the sound speed equation [*Del Grosso*, 1974] and regional historical hydrographic data, composed primarily of CTD casts acquired by the R/Vs Ocean Researcher I, II, and III from 1985 to 2010 [http://www.odb.ntu.edu.tw/], supplemented by profiles collected by Argo floats and extracted from the National Oceanographic Data Center (http://www.nodc.noaa.gov/argo/accessData.htm). Two Seagliders operated by the Applied Physics Laboratory, University of Washington, provide additional profiles collected between November 2012 and May 2013. In total 118 CTD profiles are used to determine d_{pyc} and τ_{800} for Taiwan and 798 for Luzon.

Pycnocline depth is defined here by the maximum density gradient ($d\rho/dz$) below the seasonal thermocline, calculated for each density profile located within the two regions bounded by yellow dashed lines (Figure 1), and plotted against the corresponding τ_{800} (calculated for each profile from the sound speed equation). In the mean, the pycnocline is found at sigma, $\sigma = 25.700\,\mathrm{kg\,m^{-3}}$ and 304 m depth northeast of Luzon and at $\sigma = 25.696\,\mathrm{kg\,m^{-3}}$ and 326 m depth east of Taiwan. For both the Luzon and the Taiwan regions, d_{pyc} and τ_{800} exhibit a linear relationship with correlation coefficient of 0.94 in each case (Figure S1 in the supporting information). These linear relationships are then used to derive time series of pycnocline depth from time series of PIES-measured τ_{800}.

Time series of τ_{800} and of SSHa are band-pass filtered from 30 to 180 days to isolate Kuroshio/eddy interactions. Finally, for each PIES site, lagged correlations between τ_{800} and SSHa (at each SSHa grid point) are calculated for lags varying between 0 and 100 days. Since τ_{800} is an excellent proxy for d_{pyn} (as described above), strong lagged correlations between τ_{800} at a PIES site, and the SSHa field imply a dynamical link between variations in pycnocline depth and propagating sea surface height anomalies.

3. Results

The offshoremost PIESs at both arrays record the direct influence of impinging eddies. Correlation maps comparing τ at individual PIES sites with gridded SSHa at different lags (Figure 2) reveal eddy paths from the offshore edges of the PIES arrays to the interior North Pacific as regions of high negative correlation (blue shading) whose distance from the western boundary increases with increasing lag. At zero lag, the correlations between τ and the local SSHa are strongly negative for the farthest offshore PIESs (Figures 2a and 2k)—consistent with pycnocline heaving beneath cyclones and depression beneath anticyclones. Significant negative correlation can be tracked back to 128°E, 24°N at 80 day lag off Taiwan (Figure 2e) and 128°E, 15°N at 20 day lag off Luzon (Figure 2m), corresponding to eddy translation speeds of 0.11–0.24 $\mathrm{m\,s^{-1}}$ (Taiwan) and 0.07–0.20 $\mathrm{m\,s^{-1}}$ (Luzon). For comparison, the propagation speed of Rossy waves or nonlinear mesoscale eddies is 0.08 $\mathrm{m\,s^{-1}}$ at ~20°N [*Chelton and Schlax*, 1996; *Chelton et al.*, 2011].

In contrast to these farthest offshore PIES sites, measurements from the onshoremost PIESs suggest different behavior northeast of Luzon and east of Taiwan. Northeast of Luzon, there is strong negative correlation between τ and local SSHa at zero lag (Figure 2p). However, this region of negative correlation is not apparent in the lagged maps (Figures 2q–2t), suggesting that d_{pyc} on the inshore side of the Kuroshio does not respond to eddies impinging from the interior North Pacific.

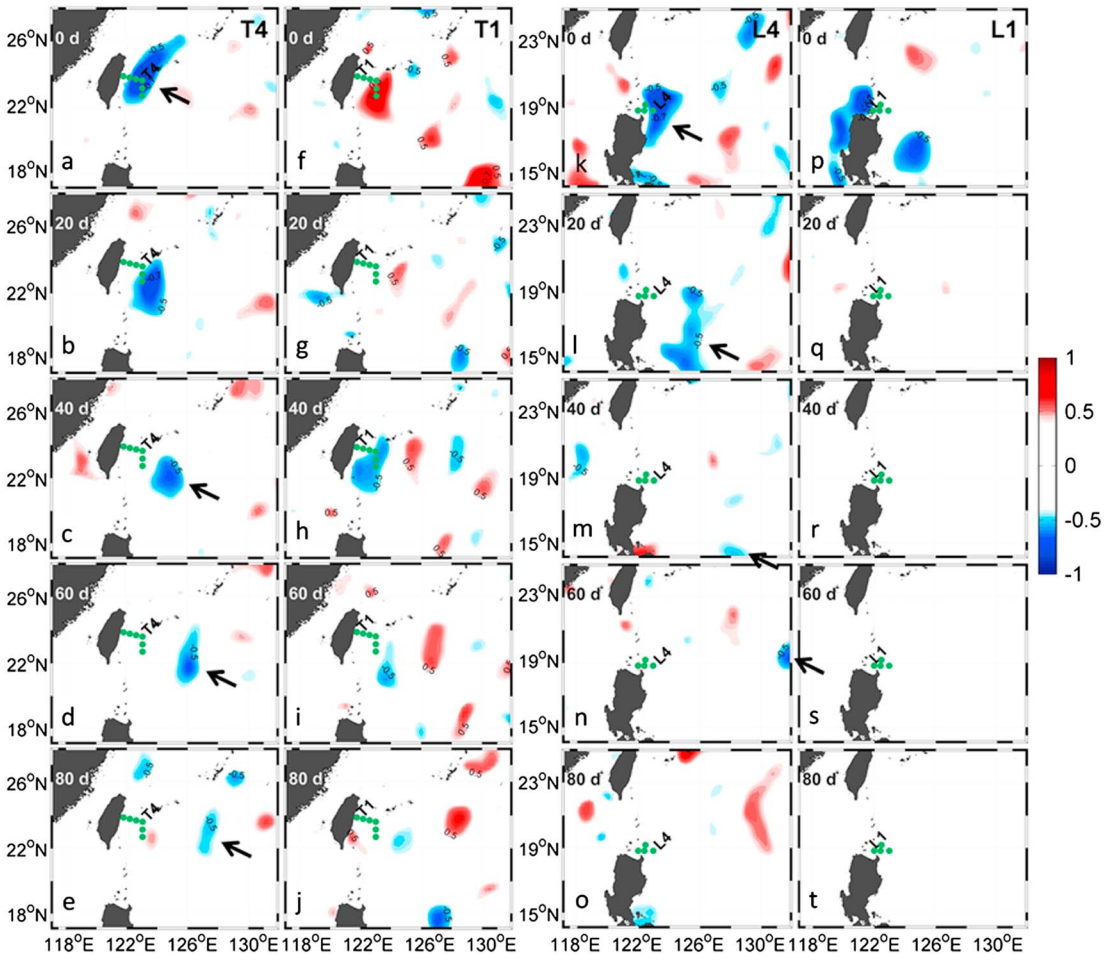

Figure 2. Maps of lagged correlations between τ at a PIES site and gridded SSHa. Columns indicate the different PIES sites, which are T4, T1, L4 and L1, respectively, from left to right. Rows indicate different time lags, which are 0, 20, 40, 60 an 80 days, respectively, from top to bottom.

Off Taiwan, the inshore side of the Kuroshio exhibits a region of positive correlation at zero lag that shifts eastward with increasing lag (Figures 2f–2j). Taken together with the pattern of negative correlations at the site on the offshore side of the Kuroshio (Figures 2a–2e), this suggests that eddies impinging east of Taiwan cause a seesaw of opposing sea level and pycnocline depth changes across the Kuroshio. Indeed, concurrent 30–180 day band-pass-filtered coastal sea level records from the Hualien tide station (Figure 1) from November 2012 through November 2014 show positive correlation with SSHa adjacent to the east coast of Taiwan but negative correlation with SSHa offshore of the Kuroshio, between 123.5 and 124.5°E, providing additional evidence of a seesaw-like response of sea level across the Kuroshio.

One possible explanation of the above mentioned responses to eddy arrivals east of Taiwan is as follows. Approaching anticyclones (positive SSHa with a depressed pycnocline in its center) depress the pycnocline on the Kuroshio's offshore side, producing negative τ anomalies, but these are limited to the region offshore of the Kuroshio's velocity maximum. There is a barrier to further onshore propagation of the eddy influence, presumably due to the Kuroshio-induced distortion and advection of the eddy before it can reach the onshore side of the Kuroshio. The anticyclone accelerates the Kuroshio by the increased isopycnal and sea surface tilts across the current. Anticyclones also drive pycnocline *heaving* inshore of the Kuroshio core (implied by the *positive* correlations in Figures 2f–2j), further amplifying isopycnal tilt and accelerating the flow. Impinging cyclonic eddies (negative SSHa and heaved pycnocline) have the opposite impact, decreasing isopycnal tilt and decelerating the Kuroshio.

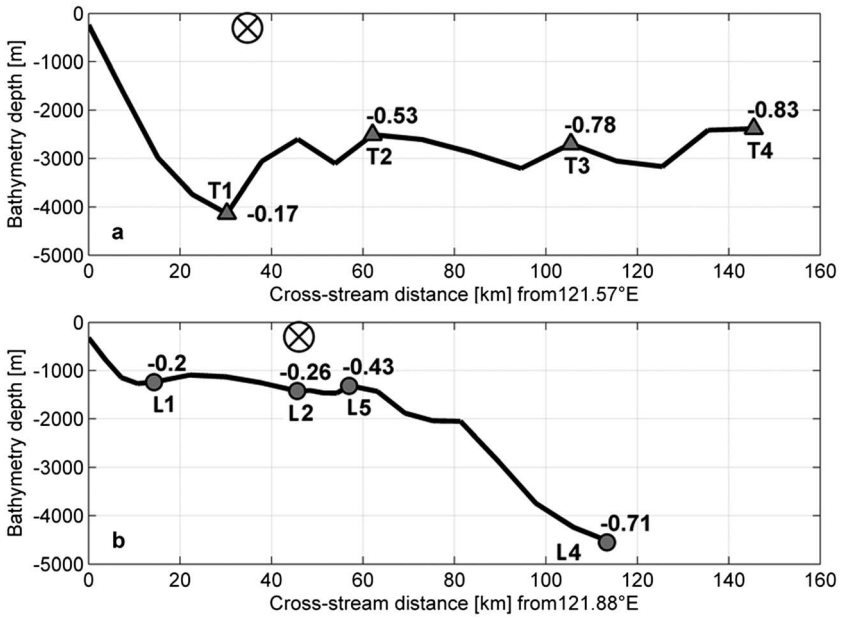

Figure 3. Bathymetry across the Kuroshio at the (a) Taiwan and (b) Luzon arrays with the zero lag correlation between τ and local SSHa indicated for each PIES site. Note that the τ record from one PIES off Luzon (site L3) is noisy and is thus excluded from the data analysis here. The mean position of the Kuroshio maximum velocity, derived from surface drifter data, is marked with a cross.

There is no evidence of a similar "seesaw" process across the Kuroshio northeast of Luzon, possibly due to differences in the onshore boundary condition (open at Luzon Strait versus a solid wall at Taiwan) or insufficient sampling that failed to fully resolve the response inshore of the Kuroshio core off Luzon.

The spatial range of the direct influence of westward propagating eddies on the Taiwan and Luzon arrays is quantified by comparing the zero lag correlations at each station between τ and local SSHa (Figure 3). Topography is not obviously related to the extent of eddy-influence, but Kuroshio position does seem to play a role. In both regions, correlation magnitude decreases only modestly between the easternmost PIES and the position of the Kuroshio velocity maximum (determined from surface drifter data, *Jan et al.* [2015]). West of the Kuroshio velocity maximum, correlation magnitude decreases sharply (see T1 versus T2 and L1 versus L5 in Figure 3).

Supplemented with the time-varying SSHa, time series of d_{pyc} on each array's offshore side (sites T4 and L4) capture the Kuroshio's response to individual eddies (Figures 4a and 4b). Seven pycnocline displacement "events" are identified east of Taiwan and nine northeast of Luzon. Note that eight of nine Luzon events are the same as those detected by *Lien et al.* [2014] who adopted a slightly different volume transport anomaly as the criterion to identify eddy influence. The corresponding SSHa (measured with altimetry) indicates that the pycnocline deepens (and τ_{800} decreases) as local SSHa increases and shoals as SSHa decreases (Figures 4a and 4b). During the observation period, d_{pyc} varies by ~125 m at east of Taiwan (T4) and ~70 m northeast of Luzon (L4). For every ±10 cm of sea surface displacement due to an eddy arrival, the pycnocline's vertical displacement is ∓32 m (∓24 m) off Taiwan (Luzon).

Eddies near the arrays are identified using the Okubo-Weiss parameter [*Isern-Fontanet et al.*, 2004; *Okubo*, 1970; *Weiss*, 1991]

$$W = \left(\frac{\partial u}{\partial x} - \frac{\partial v}{\partial y}\right)^2 + \left(\frac{\partial v}{\partial x} + \frac{\partial u}{\partial y}\right)^2 - \left(\frac{\partial v}{\partial x} - \frac{\partial u}{\partial y}\right)^2$$

This parameter measures the relative importance of deformation and rotation (relative vorticity). The SSHa system is strain dominant as $W > 0$, while vorticity is dominant as $W < 0$. To calculate W, geostrophic velocities (u, v), estimated from SSHa, are obtained from AVISO. The center of an eddy is defined at the local SSHa extrema of the eddy that is vorticity dominant, i.e., $W < 0$. After determining the center of an eddy using W, its origin is

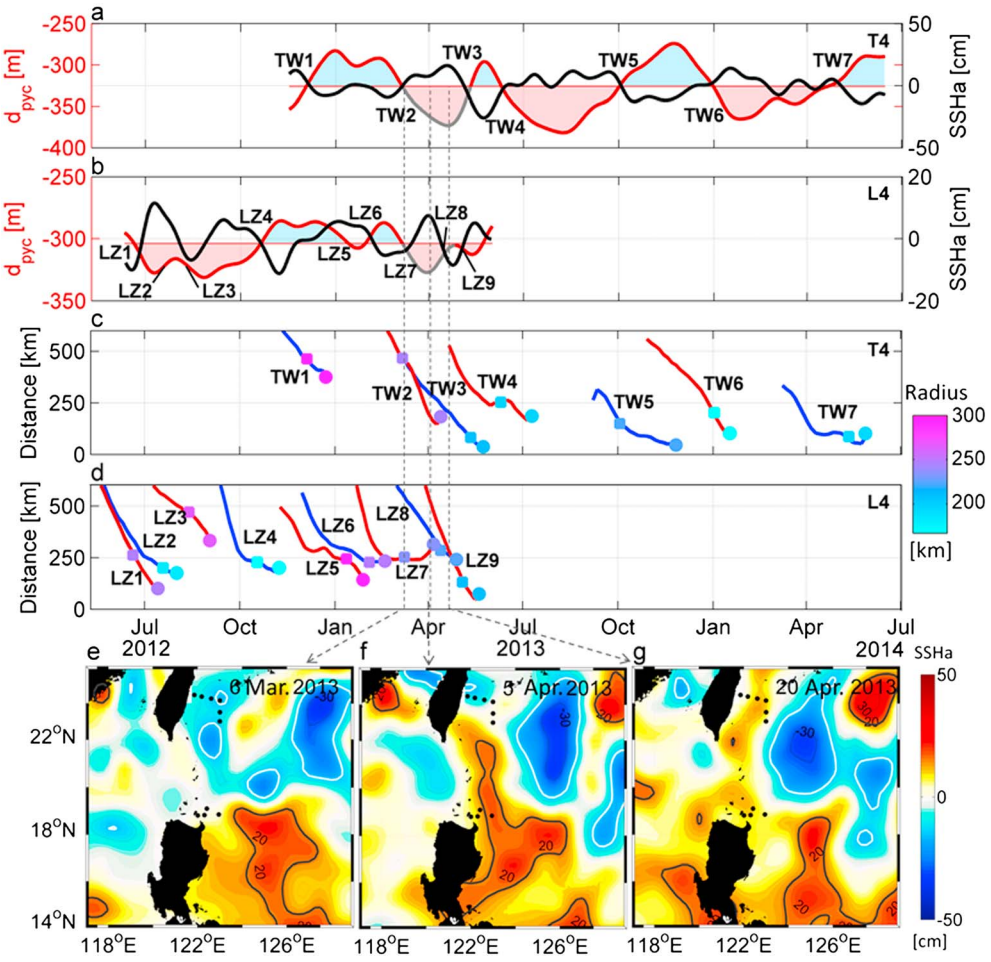

Figure 4. Time series of d_{pyc} (inferred from τ, red lines) and corresponding SSHa (measured by altimetry, black lines) at station (a) T4 and (b) L4. The time-varying distance between a propagating eddy (red lines for anticyclones and blue lines for cyclones) and the PIES location are plotted in Figure 4c for T4 and in Figure 4d for L4 and indicate the time when an eddy first begins to influence the d_{pyc} at the PIES (solid square) and when eddy influence on d_{pyc} begins to wane (solid circle). The color code on the right of Figures 4c and 4d indicates the mean radius of a detected eddy. (e–g) SSHa maps on 6 March 2013, 5 April 2013, and 20 April 2013, respectively. Bold black line and bold white line in Figures 4e–4g indicate 15 and −15 cm contours of SSHa, respectively.

identified in earlier daily AVISO SSHa maps by finding the nearest feature in which SSHa has the same sign and sits within 75 km (smaller than the typical radius of a mesoscale eddy ~100 km) of the present center, similar to the method described in *Lien et al.* [2014] and *Cheng et al.* [2014]. The 75 km search radius is determined by the spatial and temporal resolutions of the gridded AVISO SSHa, 25 km and 7 days, respectively, and typical propagating speeds of mesoscale eddies mentioned above. For each eddy that eventually arrives at the arrays' offshore edge (indicated by TW1–TW7 for Taiwan and LZ1–LZ9 for Luzon in Figure 4), the time-varying distance between the propagating eddy center and the PIES station is evaluated (Figures 4c and 4d), and the "significant influence distance"—namely the distance from which the eddy begins to significantly affect d_{pyc} at a targeted PIES station—is determined by identifying when dd_{pyc}/dt at the PIES station reaches maximum (or minimum) along the eddy's track (open squares in Figures 4a and 4d). The significant influence distance, which is a function of the radius of the impinging eddy, ranges from 100 to 450 km. The diminishing of eddy influence on d_{pyc} at T4 and L4, defined as the time when dd_{pyc}/dt reaches 0, is marked with open circles in Figures 4c and 4d. The associated interaction period of each event at T4 and L4 varies between 12 days and 54 days. Note that these periods do not necessarily represent the total timescale of the Kuroshio/eddy interaction as the eddies could be advected downstream, away from the geographically fixed PIES arrays.

Previous observations suggest that relative vorticity associated with the offshore flank of the Kuroshio is typically $-2\times10^{-5}\,s^{-1}$ in the upper 300 m (1 m s^{-1} velocity difference over a Kuroshio half width of ~50 km) and the maximum velocity of the Kuroshio ranges from 1.0 to 1.5 m s^{-1} [*Jan et al.*, 2015]. For comparison we estimate relative vorticity on the eddies' western (or leading) flanks and the associated maximum orbital velocities (Table S2). The maximum orbital velocity is 0.35–0.62 m s^{-1} for eddies that impinged on the Taiwan array and 0.32–0.79 m s^{-1} for those at the Luzon array, both smaller than the Kuroshio maximum velocity. Differences in maximum velocity between the Kuroshio and the impinging eddies likely restricts both linear and nonlinear interactions to the offshore flank of the Kuroshio, leading to deformation of eddies before they can reach across the Kuroshio maximum velocity core and advection of the SSH anomalies downstream along the Kuroshio. Moreover, eddy relative vorticity magnitude is about $0.1–1.0\times10^{-5}\,s^{-1}$, up to an order of magnitude smaller than the Kuroshio's relative vorticity on its offshore flank. An impinging eddy with comparatively weak vorticity cannot induce significant influence on the Kuroshio, and the interaction between the two systems thus occurs mainly in the Kuroshio offshore flank [*Chern and Wang*, 2005]. *Lien et al.* [2014] found that the Kuroshio's ageostrophic component northeast of Luzon is more significant on the onshore flank of the Kuroshio than on the offshore flank. The offshore Kuroshio could thus favor a significant interaction with a nearly geostrophic eddy, whereas the agoestrophic onshore Kuroshio may hardly interact with the eddy.

Generally, the d_{pyc} anomaly events coincide with the arrivals of westward propagating eddies, which cause deepening (or shoaling) of d_{pyc} associated with a positive (or negative) SSHa system (Figure 4). However, two d_{pyc} deepening events, LZ7 and TW2, marked with gray lines in Figures 4b and 4a, occurred consecutively at Luzon (L4) and Taiwan (T4), likely due to an eddy that impinged on the Luzon array from the east, but was then carried northward to impact the Taiwan array from the south. A westward moving anticyclone, originally detected by *Lien et al.* [2014], encountered the Luzon array in early March 2013 (Figure 4e), deepening the pycnocline at L4 (event LZ7 in Figure 4b). This impinging eddy was subsequently deformed and carried downstream with the Kuroshio in early April 2013 (Figure 4f). The SSHa map in late April 2013 (Figure 4g) suggests that the elongated anticyclone east of Luzon Strait reached the Taiwan array deepening the pycnocline at T4 (event TW2 in Figure 4a). Though a separate cyclone was present east of Taiwan, the pycnocline remained anomalously deep (due to the positive SSHa from the south) until early May 2013. The time lag between the two correlated d_{pyc} deepening events at Luzon and then Taiwan is approximately 21 days, suggesting advection at 0.36 m s^{-1} from L4 to T4. This speed is consistent with Kuroshio velocity at 200–400 m depths measured by shipboard acoustic Doppler current profiler (ADCP) during ship surveys east of Taiwan [*Jan et al.*, 2015] and by moored ADCPs off northeast of Luzon [*Lien et al.*, 2014]. This case suggests that d_{pyc} could be affected by SSHa systems from the south and the east. The resulting d_{pyc} variation likely depends on the relative strength of the impinging eddies.

4. Conclusions

Observations from PIES arrays located off Luzon and Taiwan suggest that Kuroshio maximum velocity—which is normally larger than the orbital velocity of eddies that impinge on the Kuroshio in this region—could influence the dynamics and deform the shape of eddies, thereby weakening the impact of eddies on pycnocline depth along the Kuroshio's western flank. Possible Kuroshio acceleration (deceleration) due to impinging anticyclonic (cyclonic) eddies increases (decreases) the magnitude of pycnocline slope across the Kuroshio, particularly east of Taiwan where impinging eddies cause seesaw-like SSHa changes across the Kuroshio. Eddies impinging on the Kuroshio east of Luzon do not generate an analogous response. The significance of ageostrophic effects on the onshore flank of the Kuroshio [*Lien et al.*, 2014] may overwhelm the indirect influence of eddies. It may also be due to the open boundary condition on the western end of Luzon PIES array, which is open to the South China Sea in contrast to the array east of Taiwan where Taiwan serves as a solid wall boundary; this merits a thorough investigation in the future.

Kuroshio pycnocline depth (d_{pyc}) along the offshore flank responds to impinging eddies, deepening (shoaling) under the influence of positive (negative) SSHa. The Taiwan (Luzon) PIES arrays capture seven (nine) d_{pyc} anomalies during their 1.5 (1) years sampling period. Eddy influence on the Kuroshio pycnocline could be felt up to 100–450 km away from the associated PIES station, depending on eddy size and strength. The duration of interactions at T4 and L4 ranged from 12 days to 54 days. During the period when both PIES arrays sampled

together (November 2012 to June 2013), three (five) d_{pyc} anomaly events occurred near Taiwan (Luzon), with one event attributed to a single eddy that impinged on Luzon from the east, and was then carried northward into the Taiwan array. The associated translation speed (L4 to T4) was estimated at 0.36 m s^{-1}.

These in situ arrays, together with idealized and realistic numerical models [*Kuo and Chern*, 2011; *Gopalakrishnan et al.*, 2013], provide a more complete view of the fate of eddies arriving along the western boundary, and of their subsequent influence on the Kuroshio. Further quantifying the energy exchange that governs Kuroshio/eddy interactions is challenging and will be the focus of future investigations using these data. Particularly, analysis of model results will focus on the evolving process and dynamics of the seesaw-like sea level and pycnocline depth variations across the Kuroshio east of Taiwan.

Acknowledgments

This study was sponsored by Ministry of Science and Technology (MOST) of Taiwan, R.O.C. grant NSC-101-2611-M-002-018-MY3 and the US Office of Naval Research (ONR) grants N00014-12-1-0445 and N00014-15-1-2593 to MA. RCL, CML, and TBS were sponsored by ONR grants N00014-10-1-0397, N00014-10-1-0308, and N00014-10-1-0468, respectively. The Ocean Data Bank of the MOST (http://www.odb.ntu.edu.tw/) provided the historical CTD and ADCP data. The drifter trajectory data were downloaded from the Coriolis Data Assembly Centers at http://www.coriolis.eu.org/Data-Services-Products/View-Download/Data-selection. The satellite sea surface height data were obtained from the Archiving, Validation and Interpretation of Satellite Oceanographic data at http://www.aviso.oceanobs.com/ducas/. Two anonymous reviewers provided constructive suggestions, which helped strengthen the interpretation of this paper. The captains and crew members of the R/Vs Roger Revelle, Ocean Researcher I, III and V, and technicians W.-H. Ho, W.-H. Lee, H.-C. Hsieh, and B. Wang assisted the deployment and recovery of PIES moorings. We thank Jeffrey Early, Northwest Research Associates, for discussions of the water mass structure within mesoscale eddies.

The Editor thanks two anonymous reviewers for their assistance in evaluating this paper.

References

Andres, M., J.-H. Park, M. Wimbush, X.-H. Zhu, K.-I. Chang, and H. Ichikawa (2008a), Study of the Ryukyu Currenpbt - Kuroshio system based on the integrated use of satellite altimetry and in situ data, *J. Oceanogr.*, *64*, 937–950.

Andres, M., M. Wimbush, J.-H. Park, K.-I. Chang, B.-H. Lim, D. R. Watts, H. Ichikawa, and W. J. Teague (2008b), Observations of Kuroshio flow variations in the East China Sea, *J. Geophys. Res.*, *113*, C05013, doi:10.1029/2007JC004200.

Baker-Yeboah, S., D. R. Watts, and D. A. Byrne (2009), Measurements of sea surface height variability in the eastern South Atlantic from pressure sensor-equipped inverted echo sounders: Baroclinic and barotropic components, *J. Atmos. Oceanic Technol.*, *26*, 2593–2609, doi:10.1175/2009JTECHO659.1.

Chelton, D. B., and M. G. Schlax (1996), Global observations of oceanic Rossby waves, *Science*, *272*, 234–238.

Chelton, D. B., M. G. Schlax, R. M. Samelson, and R. A. de Szoeke (2007), Global observations of large oceanic eddies, *Geophys. Res. Lett.*, *34*, L15606, doi:10.1029/2007GL030812.

Chelton, D. B., M. G. Schlax, and R. M. Samelson (2011), Global observations of nonlinear mesoscale eddies, *Prog. Oceanogr.*, *91*, 167–216, doi:10.1016/j.pocean.2011.01.002.

Cheng, Y.-H., C.-R. Ho, Q. Zheng, and N.-J. Kuo (2014), Statistical characteristics of mesoscale eddies in the North Pacific derived from satellite altimetry, *Remote Sens.*, *6*(6), 5164–5183, doi:10.3390/rs6065164.

Chern, C.-S., and J. Wang (2005), Interactions of mesoscale eddy and western boundary current: A reduced-gravity numerical model study, *J. Oceanogr.*, *61*(2), 271–282.

Del Grosso, V. A. (1974), New equation for the speed of sound in natural waters (with comparisons to other equations), *J. Acoust. Soc. Am.*, *56*, 1084–1091.

Gopalakrishnan, S. G., F. Marks, J. A. Zhang, X. Zhang, J.-W. Bao, and V. Tallapragada (2013), A study of the impacts of vertical diffusion on the structure and intensity of the tropical cyclones using the high-resolution HWRF system, *J. Atmos. Sci.*, *70*, 524–541, doi:10.1175/JAS-D-11-0340.1.

Guinehut, S., C. Coatanoan, A. L. Dhomps, P. Y. Le Traon, and G. Larnicol (2009), On the use of satellite altimeter data in Argo quality control, *J. Atmos. Oceanic Technol.*, *26*, 395–402, doi:10.1175/2008JTECHO648.1.

He, Y., D. R. Watts, and K. L. Tracey (1998), Determining geostrophic velocity shear profiles with inverted echo sounders, *J. Geophys. Res.*, *103*, 5607–5622, doi:10.1029/97JC03439.

Isern-Fontanet, J. E., J. Font, E. Garcia-Ladona, M. Emelianov, C. Millot, and I. Taupier-Letage (2004), Spatial structure of anticyclonic eddies in the Algerian basin (Mediterranean Sea) analyzed using the Okubo–Weiss parameter, *Deep Sea Res., Part II*, *51*, 3009–3028, doi:10.1016/j.dsr2.2004.09.013.

Jan, S., Y. J. Yang, J. Wang, V. Mensah, T.-H. Kuo, M.-D. Chiou, C.-S. Chern, M.-H. Chang, and H. Chien (2015), Large variability of the Kuroshio at 23.75°N east of Taiwan, *J. Geophys. Res. Oceans*, *120*, 1825–1840, doi:10.1002/2014JC010614.

Johns, W. E., T. N. Lee, D. Zhang, R. Zantopp, C.-T. Liu, and Y. Yang (2001), The Kuroshio east of Taiwan: Moored transport observations from the WOCE PCM-1 array, *J. Phys. Oceanogr.*, *31*, 1031–1053.

Kennelly, M. A., K. L. Tracey and D. R. Watts (2007), Inverted echo sounder data processing manual, GSO Tech. Rep., 2007–02.

Kuo, Y.-C., and C.-S. Chern (2011), Numerical study on the interactions between a mesoscale eddy and a western boundary current, *J. Oceanogr.*, *67*, 263–272.

Lien, R.-C., B. Ma, Y.-H. Cheng, C.-R. Ho, B. Qiu, C. M. Lee, and M.-H. Chang (2014), Modulation of Kuroshio transport by mesoscale eddies at the Luzon Strait entrance, *J. Geophys. Res. Oceans*, *119*, 2129–2142, doi:10.1002/2013JC009548.

Meinen, C. S. (2001), Structure of the North Atlantic Current in stream-coordinates and the circulation in the Newfoundland Basin, *Deep Sea Res., Part I*, *48*, 1553–1580, doi:10.1016/S0967-0637(00)00103-5.

Okubo, A. (1970), Horizontal dispersion of floatable particles in the vicinity of velocity singularities such as convergences, *Deep Sea Res.*, *17*, 445–454.

Qiu, B. (2003), Kuroshio Extension variability and forcing of the Pacific decadal oscillations: Responses and potential feedback, *J. Phys. Oceanogr.*, *33*, 2465–2482.

Watts, D. R., and H. T. Rossby (1977), Measuring dynamic heights with inverted echo sounders: Results from MODE, *J. Phys. Oceanogr.*, *7*, 345–358.

Weiss, J. (1991), The dynamics of enstrophy transfer in two-dimensional hydrodynamics, *Physica D*, *48*, 273–294.

Yang, Y., C.-T. Liu, J.-H. Hu, and M. Koga (1999), Taiwan Current (Kuroshio) and impinging eddies, *J. Oceanogr.*, *55*, 609–617.

Zhang, D., W. E. Johns, T. N. Lee, C.-T. Liu, and R. Zantopp (2001), The Kuroshio east of Taiwan: Modes of variability and relationship to interior meso-scale eddies, *J. Phys. Oceanogr.*, *31*, 1054–1074.